

RoboDragons 2010 Extended Team Description

Akeru Ishikawa, Takashi Sakai, Jousuke Nagai, Taro Inagaki, Hajime Sawaguchi, Yuji Nunome, Kazuhito Murakami and Tadashi Naruse

Aichi Prefectural University, Nagakute-cho, Aichi, 480-1198 JAPAN

Abstract. This paper describes the system configuration of Aichi Prefectural University's RoboDragons 2010 and related research topics. Main topic in this year is that we developed a new robot hardware. We describe it in detail here. There are some improvements in soccer software. We overview our soccer software. Our research results which will be implemented near future are described: a real time computation of dominant region and a defending strategy based on a safety region.

1 Introduction

This year's extended team description paper (ETDP) of RoboDragons2010 describes a new robot hardware, an improved software of RoboDragons 2010 system and ongoing studies.

First, robot hardware. Our current robots are the fifth generation ones in our Labs. Our team has six robots, five for competition and one for a reserve. Each robot of RoboDragons consists of four omni-directional wheels, a dribbling device, two kicking devices (for chip kick and straight kick) and the embedded computer for controlling the robot. They are controlled by a host computer next to the field. Second, software. The software on the host computer originates from the one when we made a joint team with CMU in 2004 and 2005. Many improvements have done since 2005, however, this year, noticeable improvement has not done. We overview our software centering on minor changes. Third, research related topics. Several researches on strategies have been doing these years. We introduce the real time dominant region calculation and the defending strategy based on the safety region. These techniques will be implemented in the RoboDragons system in near future.

In the following sections, we describe these topics.

2 Robots

In this section, we discuss our new robots in detail. First, we show the overview of our new robot in Figure 1.

2.1 Dimensions of robot

The robot can be packed in the cylinder with dimensions of 145 *mm* height and 178 *mm* diameter. To protect the internal circuit boards and mechanical



Fig. 1. RoboDragons new robot
(Left: with cover, Right: without cover)

devices, the robot is covered by the cardboard (see Fig. 1 left). To strengthen the cardboard, the 1.5 mm thick plastic sheet is glued.

2.2 Drive unit

The robot has 4 wheels each of which is driven by a DC brushless motor. The wheel is so called an omni-wheel. Figure 2 shows the omni-wheels moving the robot.

The DC brushless motor driving the omni-wheel is Maxon's "EC 45 flat 30 W" with encoder unit. The source voltage of the motor is 15 V. The motor also has a pinion gear with 21 teeth and the omni-wheel has a gear with 64 teeth so that the reduction ratio is 1 : 3.047. The diameter of the omni-wheel is 56 mm and the omni-wheel has 15 small tires in circumference. The diameter of the small tire is 13 mm.

2.3 Kicking device

The kicking device consists of solenoids, kick bars, and a voltage booster. Figure 3 (left) shows the kicking device and figure 3 (right) shows the voltage booster.

Solenoids Three solenoids are built in the robot, one large solenoid is for a main kick device and a small solenoid is for a chip kick device.

The coil of the large solenoid is made winding the 0.6 mm^ϕ enamelled wire on a bakelite cylinder in 7 layers. The dimensions of the cylinder are 13 mm in inner diameter, 26 mm in outer diameter and 55 mm in length. The stroke of the solenoid is 30 mm and enables the kicking a ball with speed of 9.5 msec under the ideal conditions.

The coil of the small solenoid is made using the same material with the large one. The dimension of the cylinder is 13 mm, 26 mm and 27 mm, respectively.

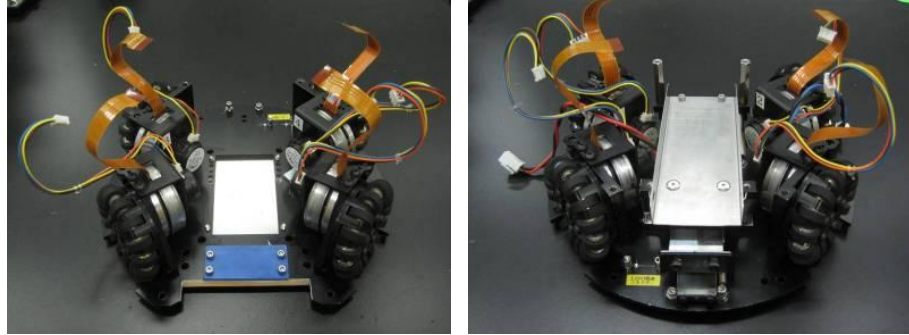


Fig. 2. Omniwheels and DC brushless motors
(Left: without solenoid, Right: with solenoid)

The stroke is 7 mm and it can kick the ball with flying distance of 2 m and flying height of 1 m.

Each solenoid employs the spring to pull back the plunger.

Kick bar 7075 aluminum alloy which is light and hard is employed for the kick bar. Moreover, V-shaped ABS plastic is attached to the aluminum kick bar as shown in figure 3. This helps to kick the ball to the direction perpendicular to the kick bar within the accuracy of 5 degree.

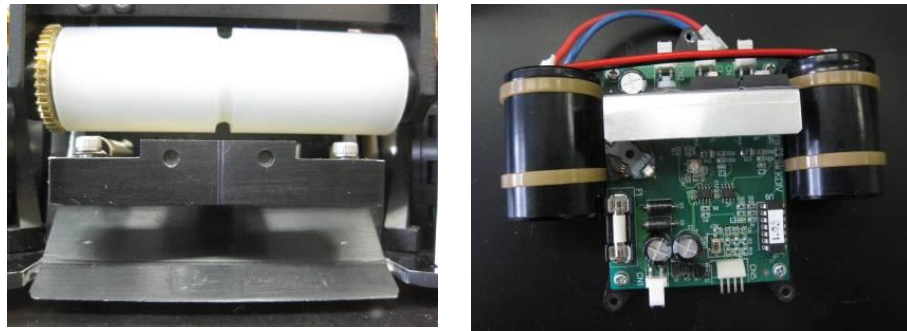


Fig. 3. Kicker and voltage booster
(Left: kicker, Right: voltage booster)

Voltage booster: The voltage booster(Fig.3(right)) is a kind of DC-DC converter. It converts 15 V DC input voltage up to 200 V DC output voltage.

Output voltage is adjustable between 150 V and 200 V. The chopper circuit using a choke coil is a heart of the voltage booster. A PIC controls the chopper circuit. Large capacity condensers are used for keeping the high voltage output. Total capacity is 4500 μF . The voltage sensing circuit controls the output voltage. 2 solid state relays are used as the switches to drive the solenoids. These relays are controlled exclusively by the PIC. The charging time of the condensers is about 2 sec when the output voltage is 200 V.

2.4 Dribbling device

A dribbling device of the robot has been achieved by combining the dribble roller, the motor and the gear.

The dribbling device uses a Maxon's "EC 16 15W" motor with an encoder and a planetary gear. The reduction ratio of the gear is 1 : 5.4. A pinion gear attached to the motor has 40 teeth and a gear attached to the dribble roller has 36 teeth. Therefore, the net reduction ratio R is given by,

$$R = R_m \times R_g = 5.4 \times \frac{36}{40} = 4.86, \quad (1)$$

where, R_m is the reduction ratio of the planetary gear and R_g is the reduction ratio of the pinion gear and the gear on the dribble roller.

The dimensions of the dribble roller are 20mm in diameter and 73mm in length. The material of the dribble roller is a aluminum shaft with silicon rubber of 4mm thickness on the face of the shaft.

2.5 Communication unit

Our wireless communication is a spectrum diffusion communication on the 2.4 GHz band. Futaba's wireless modem "FRH-SD07T" is used for the purpose. The modem has several communication modes. We use a "direct mode" which can send the messages with the least delay between modems. A pair of the FRH-SD03T and the FRH-SD07T realizes the communication between the host computer and the robot(s).

2.6 Proximity sensor unit

The proximity sensor is attached above the dribbling device and it detects the ball just in front of the dribbling device. The heart of the sensor is three infra-red light emission diode (LED) and photo diode pairs. The irradiation angle of the LED is about 15 degree. When one of the three photo diodes gets the reflected infra-red ray more than a preset threshold value, the sensor outputs the signal.

2.7 Control unit

A control unit of robot is a board computer, which is newly developed. It is shown in figure 4 These boards include a The CPU is Hitachi's SH2A processor with FPGA for peripheral control. SH2A has abundant peripheral circuits in it and makes the compact implementation of the control unit possible. The memories compose of Flash ROM(1MB) and SRAM(1MB). The IO boards have power transistors that can drive the motors and they also have interface circuits with the motors driving wheels and dribble roller, and the proximity sensor.

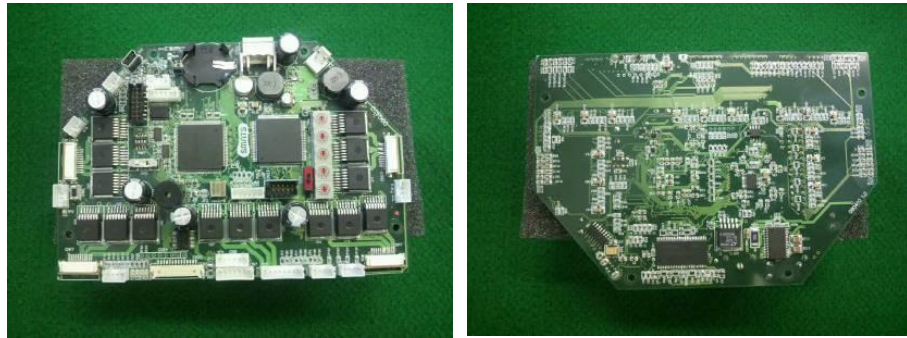


Fig. 4. Processor boards
(Left: face, Right: back)

2.8 Control program on robots

At the time this paper is written, the software shown below is not implemented on the robot yet, however, it will be implemented until RoboCup 2010 competition.

The program is written by the C programming language. The TOPPERS real time OS[1] is used.

Robot control program consists of three modules each of which is invoked as a process. They are communication, command and motor control modules. Figure 5 shows a data/signal flow among modules and peripheral units.

Robot command is sent from the host computer to robots by a packet every 1/60 seconds using asynchronous serial communication. Since the communication speed is 19200 bps in our system, it is possible to send 32 bytes data in 1/60 second if only start bit and one stop bit are used as control bits. Therefore, Our packet is consisted of 32 bytes¹ as shown in figure 6. The packet is broadcasted to all robots. The packet has error correcting code (ECC) to make reliable communication possible. We use the Humming code as the ECC.

¹ The command cycle synchronizes with the camera cycle which is equal to 59.94 frames per second. Therefore, the command can send without any problem.

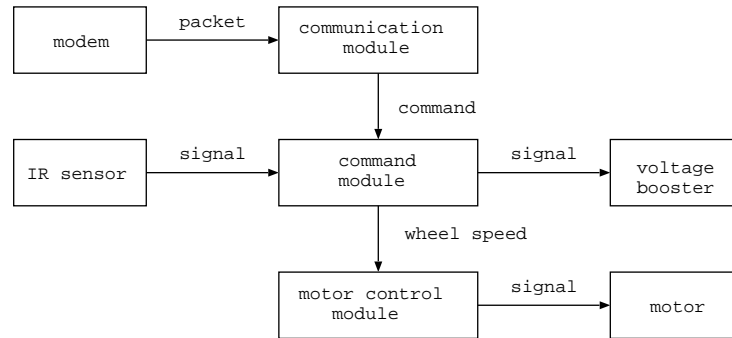


Fig. 5. Data/signal flow

The communication module receives the packet and extracts the command of its own. If error is detected, the packet is discarded. As far as the error is not burst error, the discard of packet is a good alternative². Extracted command is sent to the command module.

In the command module, the velocity of each wheel is calculated from the vel, dir and rot value (see Fig. 6) and calculated result is sent to the motor control module. The kick and dribble command is executed, as well.

In the motor control module, the PID control is performed. This is done by using the target velocity given by the command and the current velocity calculated from the encoder pulses. The motor drive control is done by the PWM control.

3 Software system

3.1 Overview

Figure 7 shows the overview of the RoboDragons system. The features of the system are as follows:

1. Host computer is Athlon64 X2 4200+ with 512MB memory and Debian GNU/Linux OS.
2. Each module(shown in box in Fig.7) is implemented as a thread.
3. The *Soccer* module consists of a strategy, a tactics and a path generation submodules, and it produces an action command for each robot.
4. *Radio* module sends the command to each robot through the radio system.

In the next sections, we describe the main improvements of our program.

² There are no such errors experienced in recent competitions.

```

class SerialCommand{
public:
    uint8_t vel;    // Velocity [unit: cm/s]

    uint8_t dir;    // Direction [unit: 2*pi/256 rad]

    uint8_t rot;    // Rotation velocity [unit: 2*pi/60 rad/s]

    uint8_t var;    // kick and dribble command
                    // b0-b1: kick condition
                    //      0 : No kick
                    //      1 : kick when center senser reacts
                    //      2 : kick when any sensors react
                    //      3 : kick immediately
                    // b2-b3 · b7: Selection of kicker
                    //      0 : No kick
                    //      1 - 4 : Main kicker (1: weak ... 4: strong)
                    //      5 - 7 : Chip kicker (5: weak ... 7: strong)
                    //      : Main and chip kickers are used exclusively
                    // b4-b5: Dribble
                    //      0 : No dribble
                    //      1 : Reverse rotation
                    //      2 : Weak normal rotation
                    //      3 : Strong normal rotation

    uint8_t ecc01;  // b0-b3: ECC of vel
                    // b4-b7: ECC of dir

    uint8_t ecc23;  // b0-b3: ECC of rot
                    // b4-b7: ECC of var
};

struct SerialPacket{
    uint8_t header0; // 0x80
    uint8_t header1; // 0x0D
    SerialCommand robot[5];
};

```

Fig. 6. Packet configuration

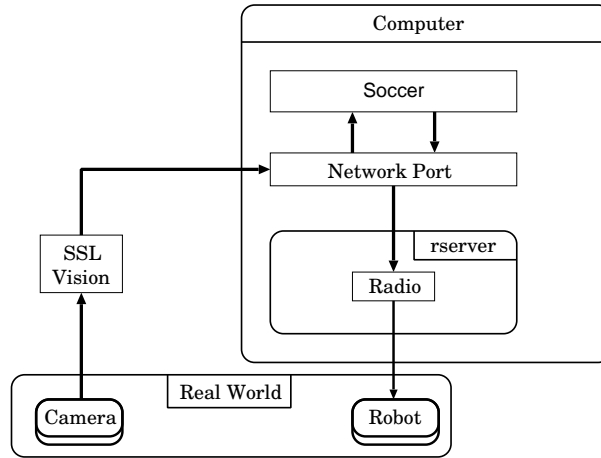


Fig. 7. RoboDragons system: overview

3.2 Determining the number of mark robots

In our old strategy, the role of each teammate robot at the opponent free kick time was determined by the ball's position. For example, if the ball is within 500 mm from teammate goal line at the beginning of the free kick, it is considered to be an opponent corner kick and "3 mark robots" strategy is selected even if an opponent robot is out of field by a penalty. The program is improved to determine the number of mark robots dynamically as follows,

Let \mathbf{r}_i be the position of the opponent robot i . If following conditions are satisfied, the robot i will be marked.

- The distance between \mathbf{r}_i and the center of teammate goal is less than R mm.
- The distance between \mathbf{r}_i and the teammate goal line is less than X mm, and there is a shoot course from \mathbf{r}_i to the goal.

In RoboDragons, $R = 3000$ mm and $X = 4600$ mm. The number of mark robots ranges from 1 to 3.

3.3 Priority of mark robots

In RoboDragons, the number of teammate robots for marking is at most 3. However, there are cases that more than 3 robot should be marked at the opponent free kick. For example, the case four opponent robots are attacking. In this case, we select three opponent robots to mark. For each opponent robot, a priority is given as follows, and higher priority robots are selected.

- the greater the distance between \mathbf{r}_i and the center of teammate goal, the higher the priority.

- the greater the affordance of the shoot course from \mathbf{r}_i , the higher the priority.

There are two mark actions, i.e. pass cut mark and shot cut mark. The pass cut mark has two variations, i.e. preventing the pass at around the passing robot and around the receiving robot. The shot cut mark is as well.

3.4 Robots' actions at free kick

In the old strategy, teammate's pass action and shot action at free kick were as follows. In the following, we use the term "direct play" [2]. The direct play is one of cooperative plays, i.e. a passing robot kicks the ball to a receiving robot, and the receiving robot shoots the ball immediately when it gets the ball.

- Pass action (passing robot in case of direct play)
 1. At time t_0 , the robot which has the greatest affordance of the shoot course is selected as a receiving robot of the pass.
 2. Passing robot moves to the waiting position \mathbf{T}_r .
 3. When passing robot arrives at \mathbf{T}_r at t_1 , it starts kicking action.
 4. After finishing the pass, passing robot waits there until the strategy change will happen.
- Shot action (shooting robot in case of direct play)
 1. Search the best place to receive the ball and move there until the passing robot will pass.
 2. After passing, the shooting robot moves to the shooting position which is computed from the velocity of the ball and current self position.
 3. Shoot the ball. If shot is failed, then next action is taken.

New actions are,

- Pass action (passing robot in case of direct play)
 1. At time t_0 , the robot which has the greatest affordance of the shoot course is selected as a receiving robot of the pass.
 2. Passing robot moves to the waiting position \mathbf{T}_r .
 3. When passing robot arrives at \mathbf{T}_r at t_1 , it starts kicking action.
 4. After finishing the pass, passing robot takes an attacker action.
- Shot action (shooting robot in case of direct play)
 1. Search the best place within the specified region to receive the ball and move there until the passing robot will pass.
 2. After passing, the shooting robot moves to the shooting position which is computed from the velocity of the ball and current self position.
 3. If there are some candidates for shooting, the robot nearest to the teammate goal judges the possibility of shot. If it is not possible, then take a defending action.

In the RoboDragons 1-2-3 shot[2] using three robots, above shot action works well to reduce the time the goal keeper defends the goal without any other defender(s).

4 Realtime dominant region computation

4.1 Need of realtime dominant region computation

It is important to analyze the actions of opponent team in real time and then to change team's strategy dynamically in order to overcome the opponent, since the strategies based on them are growing year after year [3]. For such analysis, the *voronoi diagram* [4] and the *dominant region diagram* [5] are useful. They are used to analyze the sphere of influence. The voronoi diagram divides the region based on the distance between robots, while the dominant region diagram divides the region based on the arrival time of robots. It is considered that the dominant region diagram shows an adequate sphere of influence under the dynamically changing environment such as a soccer game.

In the SSL, the dominant region diagram has been used for arranging team-mate robots to perform the cooperative play such as passing and shooting [2][6]. However, the existing algorithm takes much time to compute the dominant region diagram, the use of the algorithm is restricted to the case that the computation time can keep, i.e. a typical case is a restart of play. If the dominant region diagram can be computed in real time, we can apply it any time.

In this section, we describe the realtime computation of dominant region. In our system, it is required to compute the dominant region diagram within 5 msec. So, we put this time to be our present goal. Following algorithm is an approximate computation of the dominant region diagram so that we discuss the computation time and the approximation accuracy through the experiment. Our algorithm achieves 1/1000 times shorter in computing time compared with the algorithm proposed in literature [5] and over 90% accuracy. Moreover, 5 msec computation time can be possible under the parallel computers. We also show that the dominant region diagram is useful for the prediction of success for passing.

4.2 Computation of dominant region

A dominant region of an agent³ is defined as "a region where the agent can reach faster than any other agents". A dominant region diagram, simply a dominant region, shows the dominant region of every agent [5]. The dominant region diagram is one of the generalized voronoi diagrams. Though the dominant region diagram is an n dimensional diagram in general, we discuss a two dimensional diagram here because we consider a soccer field.

The dominant region is calculated as follows. Assume that an agent i is at the point $\mathbf{P}^i(= (P_x^i, P_y^i))$ and is moving at a velocity $\mathbf{v}^i(= (v_x^i, v_y^i))$. Assume also that the agent can move to any direction and its maximum acceleration is $\mathbf{a}_\theta^i(= (a_{\theta_x}^i, a_{\theta_y}^i))$ for a θ -direction. The position that the agent will be after t

³ We call a considering object (such as a player) an agent.

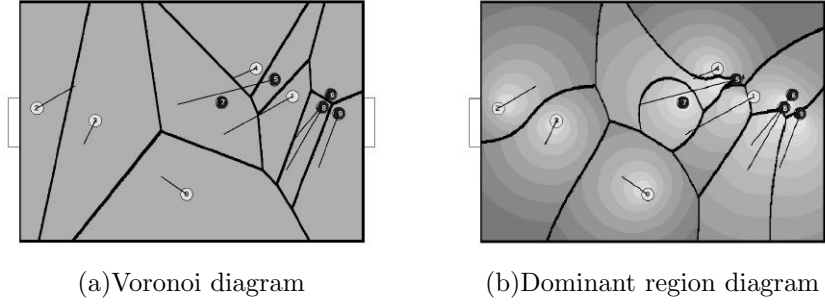


Fig. 8. Voronoi diagram vs. dominant region diagram

seconds is given by⁴,

$$\begin{pmatrix} x_\theta^i \\ y_\theta^i \end{pmatrix} = \begin{pmatrix} \frac{1}{2}a_{\theta x}^i t^2 + v_x^i t + P_x^i \\ \frac{1}{2}a_{\theta y}^i t^2 + v_y^i t + P_y^i \end{pmatrix}. \quad (2)$$

For given t , the set of above points makes a closed curve with respect to θ . Conversely, for given point $\mathbf{x} = (x, y)$, we can compute the time which each agent takes⁵. Therefore, for each point \mathbf{x} in a region (or a soccer field), we can get the dominant region by computing the following equation,

$$I_x = \underset{i}{\operatorname{argmin}}\{t^i(\mathbf{x})\}, \quad (3)$$

where, I_x is an agent's number which comes at first to the point \mathbf{x} .

Preliminary experiment using the algorithm proposed in [5] shows that the computation time takes 10 to 40 seconds when the soccer field is digitized by 610×420 grid points.

5 Approximate dominant region

To achieve a real-time computation of the dominant region, where the real time means a few milliseconds here, we propose an *approximate dominant region*. It can be obtained as a union of *reachable polygonal regions*. A reachable polygonal region is a polygon which is uniquely calculated when the motion model and time are given.

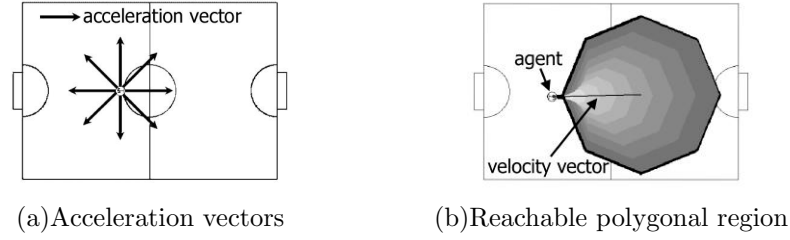


Fig. 9. Acceleration vectors and reachable polygonal region

5.1 Motion model of robots

We define a motion model as a set of maximum acceleration vectors of a robot. Figure 9(a) shows an example of a motion model. Each maximum acceleration vector shows that the robot can move to that direction with the given maximum acceleration. This is an example of an omni-directional robot. Eight vectors are given. The number of vectors depends on the accuracy of obtaining the dominant region.

5.2 Computation of reachable polygonal region

The reachable polygonal region is a region that is included in the polygon made by connecting the points, where each point is given as a point that an agent arrives at after t seconds when it moves toward the given direction of maximum acceleration vector in maximum acceleration. Eq. (2) is used to compute the point. Figure 9(b) shows an example of reachable polygonal region (shaded area) after 1 second passed when the acceleration vectors of figure 9(a) is given. We assume the reachable polygonal region is convex⁶. The reachable polygonal region is calculated by the following algorithm.

[Reachable polygonal region]

Step 1 Give a motion model of each agent (figure 9(a)).

Step 2 Give time t . Calculate each arrival point $(x_{\theta}^i, y_{\theta}^i)$ according to the equation (2) using the corresponding maximum acceleration vector in Step1.

Step 3 Connect points calculated in Step2 (figure 9(b)).

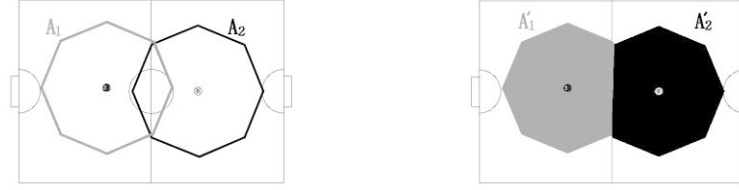
5.3 Calculation of approximate dominant region

The approximate dominant region is obtained from the reachable polygonal regions for every agent. When some of reachable polygonal regions are overlapped,

⁴ These equation do not consider the maximum velocity of the agent. If the maximum velocity must be considered, the equations should be replaced to the non-accelerated motion equations after reaching the maximum velocity.

⁵ If more than one arrival time are obtained at point \mathbf{x} for the agent i , the minimal arrival time is taken.

⁶ If it is concave, we consider a convex hull of it.



(a) Overlapped reachable polygonal regions

(b) Divided reachable polygonal regions

Fig. 10. Division of two overlapped Reachable polygonal regions

we have to decide which agent, the point belongs to the overlapped region. Figure 10(a) shows two overlapped reachable polygonal regions (A_1, A_2) of two agents. In this case, it is natural to divide overlapped region into two by the line connecting the points of intersection of two polygons. Figure 10(b) shows a result for the reachable polygonal regions. However, since the number of points of intersection between two polygons (with n vertices) varies from 0 to $2n$, we have to clarify the method of division for each case. Moreover, we need to consider the method of division when many reachable polygonal regions are overlapped. We describe these methods in the following algorithm. We call this an algorithm of the approximate dominant region.

[Approximate dominant region]

Step 1 For given time t , make a reachable polygonal region of each agent. (Figure 9(b)).

Step 2 For two reachable polygonal regions, if they are overlapped, divide the overlapped region in the following way. Generally, a number of points of intersection between two polygons with n vertices varies from 0 to $2n$. If a vertex of one polygon is on the other polygon, move the vertex infinitesimally to the direction where the number of points of intersection does not increase. (There is no side effect with respect to this movement.) Therefore, the number of points of intersection is even. We show the way to divide in case of 0, 2 and $2k$ intersections.

1. No points of intersection: There are two cases.
 - (a) Disjoint: As two reachable polygonal regions are disjoint, there is no need to divide.
 - (b) Properly included: One includes the other. Figure 11(a) shows an example ($A_1 \supset A_2$). In this case, $A_1 - A_2$ is a dominant region of agent 1 (Fig. 11(b)) and A_2 is a dominant region in agent 2 (Fig. 11(c))⁷.
2. 2 points of intersection: The overlapped regions of A_1 and A_2 is divided into two region by the line connecting the points of intersection between two polygons to create dominant regions A'_1 and A'_2 (Figure 10).

⁷ This is not correct definition, but we adopt this to perform the real time computation.

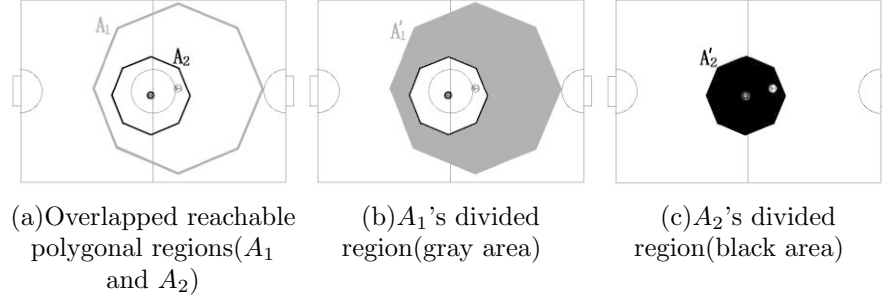


Fig. 11. Division of overlapped reachable polygonal regions (one-contains - other case)

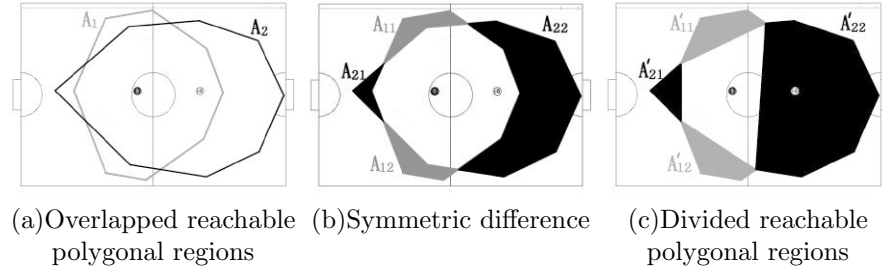


Fig. 12. Division of overlapped reachable polygonal regions (4 intersecting case)

3. $2k$ points of intersection: Let A_1 and A_2 be two reachable polygonal regions and I be a set of points of intersection between the polygons of A_1 and A_2 . Then, compute $A_1 - A_2$ and $A_2 - A_1$. Figure 12(a) shows an example. In this example, there are 4 points of intersection. Figure 12(b) shows a difference between two regions, where $A_1 - A_2 (= \{A_{11}, A_{12}\})$ is shaded in grey and $A_2 - A_1 (= \{A_{21}, A_{22}\})$ is shaded in black. Make convex hulls of subregions. Figure 12(c) shows the result ($A'_{11}, A'_{12}, A'_{21}, A'_{22}$). Thus, we have *partial dominant regions* ($A'_1 = A'_{11} \cup A'_{12}$ and $A'_2 = A'_{21} \cup A'_{22}$) of the agent 1 and 2. A white area in the overlapped region in figure 12(c) doesn't belong to either of two partial dominant regions.

Step 3 If n reachable polygonal regions (A_1, A_2, \dots, A_n) are overlapped, we process as follows. First, for A_1 and A_2 , we take partial dominant regions A'_1 and A'_2 by using the procedure in step 2. Replace A_1 and A_2 with A'_1 and A'_2 . Then, for A_1 and A_3 , and A_2 and A_3 , do the same computation. Repeat this until A_n is computed. As a result, we get new reachable polygonal regions (A_1, A_2, \dots, A_n) where any two A_i s are disjoint. These are the partial dominant regions of agents at given time t . Figure 13 shows three examples of partial dominant regions of 10 agents at time $t = 0.5, 0.7$ and 0.9 seconds.

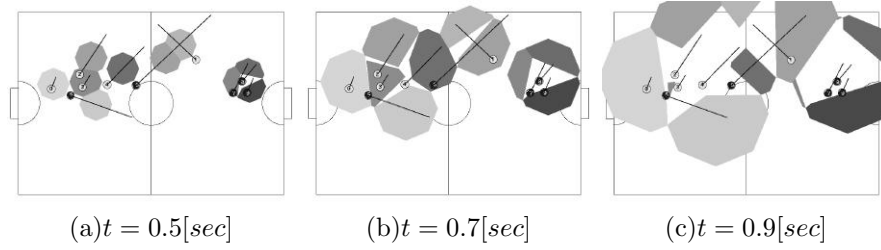


Fig. 13. Synthesis of reachable polygonal regions

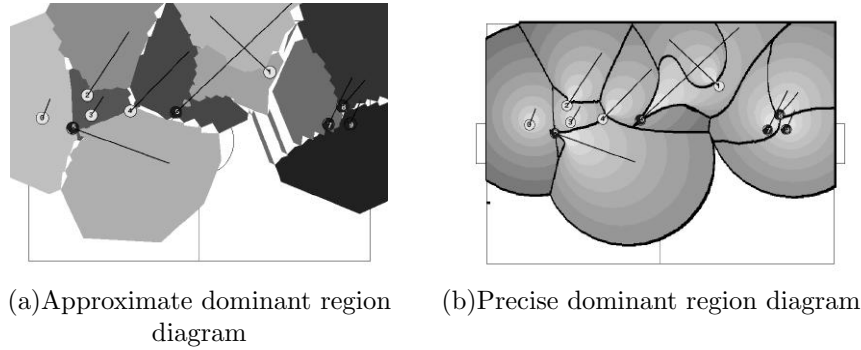


Fig. 14. Approximate dominant region diagram vs. dominant region diagram

Step 4 Synthesize the partial dominant regions incrementally. For given times t_1, t_2, \dots, t_n ($t_1 < t_2 < \dots < t_n$), compute the partial dominant regions. Let them be B_1, B_2, \dots, B_n . Then, compute $B_1 + (B_2 - B_1) + \dots + (B_n - \sum_{i=1}^{n-1} B_i)$. This makes an approximate dominant region diagram. Figure 14(a) shows an example constructed from the examples shown in figure 13, but using 10 partial dominant regions computed by every 0.1 seconds.

6 Experimental evaluation for algorithm of approximate dominant region

6.1 Experiment

In the SSL, since the ball moves very fast, the standard processing rate is 60 processings per second. One processing includes an image processing, a decision making, action planning, command sending and so on. Therefore, the allowed time for the computation of the dominant region is at most 5 milli-seconds⁸. Our purpose is to make the computation of the approximate dominant region within 5 msec.

⁸ This time constraint is sufficient when our algorithm will be applied for the other leagues in RoboCup soccer and human soccer.

Table 1. Computation time and accuracy of proposed algorithm

acc. vectors	arrival-time steps	computation time[msec]	accuracy[%]
8	10	17.5	91.8
8	20	33.8	92.9
16	10	31.4	95.3
64	200	2.4×10^3	99.9
2048	400	5.0×10^5	100

Table 2. Computation time on various computers (parameters: max acc. vectors: 8, arrival-time steps: 10)

	CPU	proposed method(A)	existing method(B)	rate(B/A)
1	3.16GHz	17.5[msec]	13.3[sec]	760
2	3.2GHz	19.3[msec]	24.2[sec]	1254
3	2.2GHz	38.2[msec]	40.5[sec]	1060
4	2.2GHz	38.3[msec]	40.4[sec]	1055

6.2 Experimental result

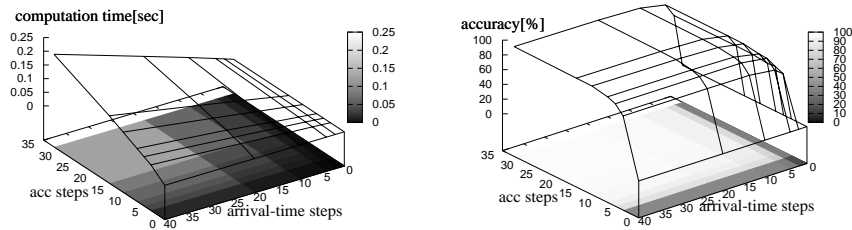
We digitize the SSL’s field into 610×420 grid points (1 grid represents the area of about 1 cm^2) and, for 10 agents (5 teammates and 5 opponents), compute the approximate dominant region that can arrive within 1 second. The reason why we set arrival time to 1 sec is that almost all of the whole field can be covered by the dominant region as shown in Fig. 14. We measure the computation time and the accuracy of the approximate dominant region. We define the accuracy by the following equation,

$$\text{Accuracy}[\%] = \frac{\text{Total grid points that } I_x^d \text{ and } I_x^a \text{ coincide}}{\text{All grid points}} * 100 \quad (4)$$

where, I_x^d and I_x^a are given by Eq. (3) for the precise dominant region and the approximate dominant region, respectively.

We used the computer with Xeon X5460 as CPU, 8GB main memory and FreeBSD operating system for this experiment. We measured the computation time by running the program in a single thread.

The computation time and the accuracy of the approximate dominant region depend on the number of maximum acceleration vectors and the number of partial dominant regions (i.e. the number of time-divisions). We measured the computation time and the accuracy for the various values by using two parameters above. Figure 15 shows the results of the measure. Table 1 shows the computation time and the accuracy for some typical values of the parameters. The resulting approximate dominant region of the first row of the Table 1 is shown in Figure 14(a).



(a) Computation time vs. acceleration vector and arrival-time step pairs (b) Accuracy vs. acceleration vector and arrival-time step pairs

Fig. 15. Computation time and accuracy

In comparison with Fig. 14(b), it is considered that Fig. 14(a) is a good approximation of the dominant region diagram. The accuracy is ranging from 91.8% to 100% from Table 1. These numbers show that our algorithm gives a good approximate dominant region.

Table 2 shows the computation time of the approximate dominant region diagram measured on the various computers. (The parameters on this experiment are fixed as the number of maximum acceleration vectors takes 8 and the number of time-divisions takes 10.) From the table, it is shown that the computation time can be reduced about 1/1000 times shorter compared with the algorithm shown in [5] and the accuracy keeps a little more over 90%. In addition, it is shown that, from Fig. 15(a), the computation time increases in proportion to the number of maximum acceleration vectors and the number of time-divisions, and from Fig. 15(b), the accuracy goes up rapidly to be 90% according to the increase of the number of maximum acceleration vectors and/or time-divisions, and then still slightly increases.

6.3 Discussion

From Table 1, the approximate dominant region with parameters of 8 maximum acceleration vectors and 10 time-divisions achieves the accuracy of 92%. However, its computation time takes 17.5 *msec*. It is a little bit far from our goal, which is computation time to be 5 *msec*. To achieve this goal, we discuss a parallel computation here. Another issue whether the accuracy of 92% is enough in our purpose will be discussed in the next section.

In our algorithm, we create an approximate dominant region by synthesizing the partial dominant regions incrementally. Each partial dominant region can calculate independently and its computation time is almost equal for all the partial regions. The latter is supported by the fact that the computation time doubles when the partial dominant regions double. (See Fig. 15(a).) And also Table 3 shows an average time to compute a partial dominant region. For synthesis of 10 partial dominant regions, it takes 0.5 *msec* on average. Therefore,

Table 3. Computation time necessary to make and to synthesize reachable polygonal regions

acc. vectors	8	16	24	32
average computation time [<i>msec</i>]	1.71	3.10	4.37	5.46
standard deviation [<i>msec</i>]	0.016	0.017	0.014	0.014

it is expected in parallel computation that the computation time will be about $1.71 + 0.5 + \alpha$ *msec* when 10 partial dominant regions are synthesized, where α is an overhead of the parallel computation and is considered as a constant. In the multi-core parallel computer, the α is small enough. We consider that it is possible to make the computation time within 5 *msec*, which is our goal.

7 Prediction of success for passing

One application of the dominant region is the prediction of success for passing. In this section, we introduce a dominant region of a ball. The approximate dominant region takes a significant role to predict the success for passing. If we can predict the success of passing accurately in real time, we can choose a defense or an offense strategy appropriately.

7.1 Approximate dominant region of ball

We consider a dominant region of a ball. The motion of the kicked ball on the SSL's field can be considered as a uniform decelerated motion, since the ball receives the force by the friction of the field only, and the friction is constant over the field. In addition, the ball moves on a straight line unless it meets with an object. Thus, the dominant region of a ball is defined as a line segment that the ball does not meet with any agents. By using the following way, it is possible to find an agent who can get the ball first: 1) compute a partial dominant region for time t_i and draw the position of ball at time t_i on it. 2) If the ball is in the dominant region of an agent, then the agent can get the ball. if not, repeat computation for next time t_{i+1} until the ball is in the dominant region of an agent. By this way, we can predict the agent who gets the ball first, and also we can find a dominant region of a ball.

Figure 16 shows an example. Fig. 16 (a) is a current situation of the game. The ball is at the lower part of the left side from the center line. The lines in front of the agents and the ball show the velocity of them. Figs. 16 (b) and (c) are the synthesized partial dominant region until $t = 0.45sec$ and $t = 0.5sec$, respectively. In Fig. 16 (b), there is no agent who can get the ball, but in Fig. 16 (c), the agent No. 4 can get the ball, since the ball is in the dominant region of the agent 4. Fig. 16 (d) shows the approximate dominant region until $t = 1sec$ and the ball's dominant region. To make this diagram, it takes 0.5 *msec* more time than the computation time of the diagram without the ball.

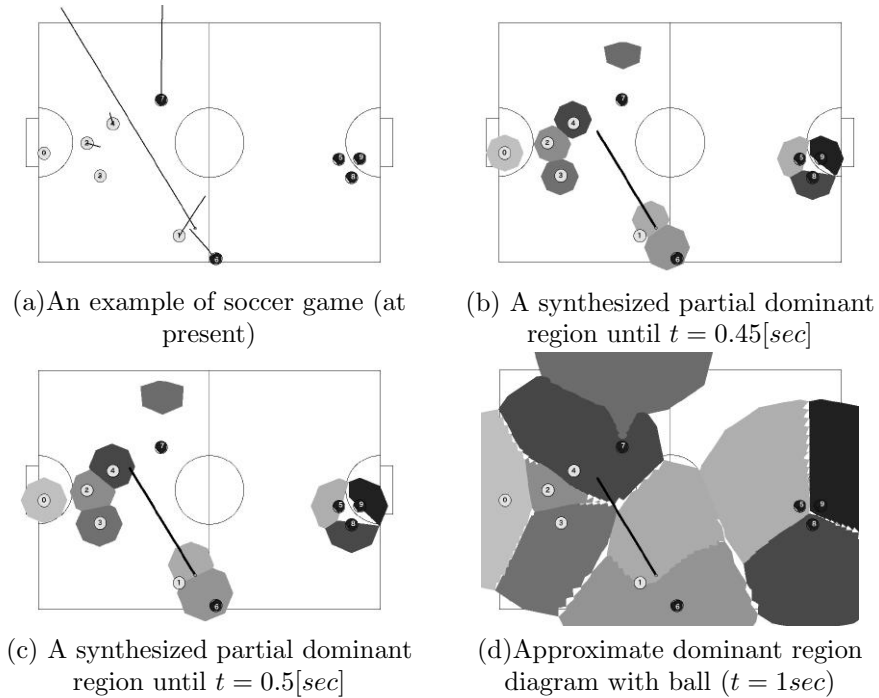


Fig. 16. Example of approximate dominant region diagram with ball

7.2 Discussion

In this experiment, we use the approximate dominant region with parameters of 8 maximum acceleration vectors and 20 time-divisions for 1 second interval⁹. We used the logged data of the third-place match in 2007 RoboCup competition to analyze the prediction of success for passing. By using the proposed algorithm, we predict the robot who gets the ball first. 60 passings are predicted correctly out of 63 total passings in the game (95% accuracy), i.e. the predicted agent and the agent that gets the ball in the game coincide.

In the results, 3 passings are failed to predict correct agents. The detailed analysis shows that the cause of mis-prediction is not due to the accuracy of the approximate dominant region but due to the strategy of the team. That is, the mis-predicted agent acts to achieve an other goal like moving the goal area to defend the goal by the team's strategy instead of getting the ball. Therefore, we think the approximate dominant region is very useful to judge the prediction of success for passing as well as to evaluate the team's strategy.

⁹ It is possible to obtain the approximate dominant region within 5 msec under the parallel computation environment even if these parameter values are used.

8 Safety region

One more topic is a safety region index. This is used for evaluating the situation of a game and deciding the defence robots where to deploy.

8.1 Definition of safety region

A concept of “safety region” is simple. It is defined as a region that the teammate robot(s) can keep the goal when an opponent robot shoots the ball from the inside of the safety region if teammates are positioned properly according to their defence strategy. Remaining region of the field given by removing the safety region is called “unsafety region”.

In the following discussion, as a first step, we do not consider the chip shot or the curved shot in the following discussion.

8.2 Calculation of safety region

The calculation of the safety region depends on how the shot action is taken, i.e. a single shot or a cooperative shot, and how the team keeps the goal, i.e. defence strategy and the number of defence robots. It takes much time to compute the precise safety region. Therefore, in the following, we describe procedures to compute the approximate safety region.

Calculation of approximate safety region: single shot case Defence robots will move according to their strategy so that we assume the right positions of the defence robots are given at any time. Let \mathbf{b} be the position of the ball at time t . Let \mathbf{r}_i be the position of the defence robot i at time t . Let L_r and L_l be the lines connecting \mathbf{b} and the right and left goalposts, respectively. (See figure 1.) Defence robots usually stand on the inside of the region the lines L_r and L_l make. Let $\mathbf{p}_{r,i}$ be the cross-point between the line L_r and the line perpendicular to L_r through \mathbf{r}_i , and let $\mathbf{p}_{l,i}$ be the cross-point similarly defined for the line L_l and \mathbf{r}_i . Assuming $\|\mathbf{r}_i - \mathbf{p}_{j,i}\| \geq R$, where $\|\cdot\|$ means a length of a vector \cdot , calculate the following equations for each defence robot i .

Compute,

$$t_s = \frac{\|\mathbf{b} - \mathbf{p}_{j,i}\|}{v_s}, \quad t_i = \frac{v_i}{a_i}, \quad (5)$$

where t_s means the time for the ball to move from \mathbf{b} to $\mathbf{p}_{j,i}$ by the speed v_s and t_i the time for the speed of robot i to be v_i (starting from speed 0). v_i and a_i are the velocity and acceleration of the defence robot, and their values are decided depending on the defence strategy.

If $t_i > t_s$, then compute whether equation

$$\frac{\|\mathbf{b} - \mathbf{p}_{j,i}\|}{v_s} > \sqrt{\frac{2(\|\mathbf{r}_i - \mathbf{p}_{j,i}\| - R)}{a_i}}, \quad (j = r, l) \quad (6)$$

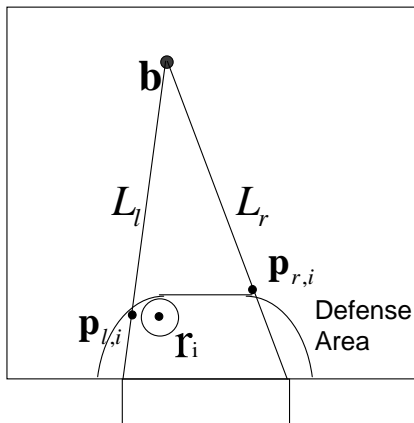


Fig. 17. Definition of the safety region: single shot case

is satisfied or not, otherwise compute whether equation

$$t_s > t_i + \frac{\|\mathbf{r}_i - \mathbf{p}_{j,i}\| - R - \frac{a_i t_i^2}{2}}{v_i}, \quad (j = r, l). \quad (7)$$

is satisfied or not, where v_s , a_i , v_i and R are the kicked speed of the ball, the maximal acceleration and velocity of the defence robot i , and the sum of radii of the defence robot and the ball, respectively.

When Equation (6) or (7) is satisfied for $j = r$ and l , the position of the ball \mathbf{b} is defined as a point in the safety region. In case there are more than one defence robot, if at least one of them satisfies Eq. (6) or (7), \mathbf{b} is defined as a point in the safety region. When $\|\mathbf{r}_i - \mathbf{p}_{j,i}\| < R$ is satisfied, \mathbf{b} is also defined as a point in the safety region.

Calculation of approximate safety region: cooperative shot case When the two opponent robots make the shot cooperatively, a typical example is a direct play[2] which is an action that shooting robot kicks the ball immediately after receiving it from a passing robot (figure 2), we have to take the passing robot into consideration since the defence robots keep their goal at the positions that defend against the attack of both robots. In this case, we have to take the passing time into consideration to compute the safety region.

Let \mathbf{b} and \mathbf{e} be the positions of the ball and the shooting robot at time t , respectively, and \mathbf{r}_i be the position of each defence robot i at time t . Let L'_r and L'_l be the lines connecting \mathbf{e} and the right goalpost and \mathbf{e} and the left goalpost, respectively. (See figure 2.) We assume the goalkeeper stands in the defence area and moves along the defence area and other defence robots stand outside defence area and move along the defence area. Then, let $\mathbf{p}_{r,i}$ be the cross-point between

the line L'_r and the line perpendicular to L'_r through \mathbf{r}_i , and let $\mathbf{p}_{l,i}$ be the cross-point similarly defined for the line L'_l and \mathbf{r}_i . Assuming that the passing robot holds the ball a obtained for cor

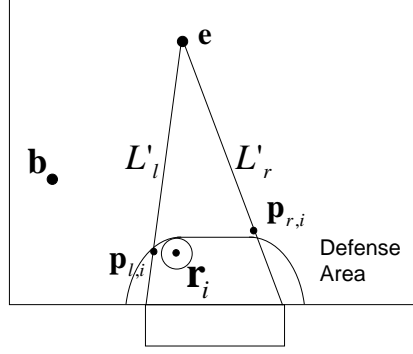


Fig. 18. Definition of the safety region: cooperative shot case

Compute,

$$t_p = \frac{\|\mathbf{e} - \mathbf{b}\|}{v_p}, \quad t_s = \frac{\|\mathbf{p}_{j,i} - \mathbf{e}\|}{v_s}, \quad t_i = \frac{v_i}{a_i}, \quad (8)$$

where t_p means the passing time between \mathbf{b} and \mathbf{e} , t_s and t_i are the same ones in Eq. (5).

If $t_i > t_p + t_s$, then compute whether equation

$$t_p + t_s > \sqrt{\frac{2(\|\mathbf{p}_{j,i} - \mathbf{r}_i\| - R)}{a_i}}, \quad (j = r, l) \quad (9)$$

is satisfied or not, otherwise compute whether equation

$$t_p + t_s > t_i + \frac{\|\mathbf{p}_{j,i} - \mathbf{r}_i\| - R - \frac{a_i t_i^2}{2}}{v_i}, \quad (j = r, l) \quad (10)$$

is satisfied or not, where, v_p , v_s , v_i , a_i and R are the speed of the ball at passing, the speed of the ball at shooting, the maximal velocity and acceleration of the defence robot i and the sum of radii of the defence robot and the ball, respectively.

If equation (9) or (10) is satisfied or there is no pass line¹⁰ between \mathbf{b} and \mathbf{e} , \mathbf{e} is a point in the safety region. In case there are more than one defence robot, if at least one of them satisfies Eq. (9) or (10), \mathbf{e} is a point in the safety region. When $\|\mathbf{p}_{j,i} - \mathbf{r}_i\| < R$, \mathbf{e} is also a point in the safety region.

¹⁰ The length of the perpendicular from \mathbf{r}_i to the line connecting \mathbf{b} and \mathbf{e} is less than the radius of the robot, it can block the pass.

9 Experiment of safety region

In this section, we show the experimental results of the safety region for the direct play[2]. We use the defence strategy of RoboDragons[7] here since we know all its details.

9.1 Method of experiment

The safety region should be calculated analytically, however, it is hard to do the analytic computation so that we calculate it on each of the mesh points which are given by dividing the field every 40 mm, and we give the approximate safety region using the model discussed in section 8.2.

On the other hand, to testify the correctness or preciseness of the proposed safety region, we compared the proposed safety region with the result of simulation, where simulation was done by using the game simulator embedded in the RoboDragons system. Here we show a simulation procedure for the cooperative play in the followings.

1. Divide the field into n mesh points, where $n = 14888$ in this experiment. Put the ball on the initial position \mathbf{b} , one of the mesh points. Also put the attacking robots on the mesh points, one around the ball and the other one a given point \mathbf{e}_i , a shooting position¹¹. Place defence robot(s) on defending position(s) according to the strategy algorithm of the RoboDragons system.
2. At time t , move the ball from \mathbf{b} to \mathbf{e} with the passing velocity v_p .
3. Move the ball on the shooting line from \mathbf{e} which is the farthest line to the defence robots when the ball arrives at shooting position \mathbf{e} at time t_e . (Shooting line is calculated at time t .)
4. Simulate the movement of the defence robots and judge if a goal is achieved or not. If the goal is achieved, then the point \mathbf{e} is a point in the unsafety region, otherwise it is a point in the safety region.
5. Repeat steps 2 ... 4 for each point in the mesh by replacing \mathbf{e} into it.

The initial position of the ball used in the simulation is selected from the logged data of the 8 games held in RoboCup Japan Open 2009 and RoboCup 2009, i.e. kick off, direct and indirect free kick points are the candidates of the initial position of the ball, and it is randomly selected from the candidates. Passing velocity and shooting velocity of the ball are 4.0 m/sec and 8.0 m/sec, respectively, which are the typical values in the SSL. The acceleration and velocity of the defence robot are 2.0 m/sec² and 0.6 m/sec, respectively, which are the measured values.

9.2 Experimental results

Coincidence rate We compared the approximate safety region with the one obtained by the simulation for the one defence robot case and the two defence

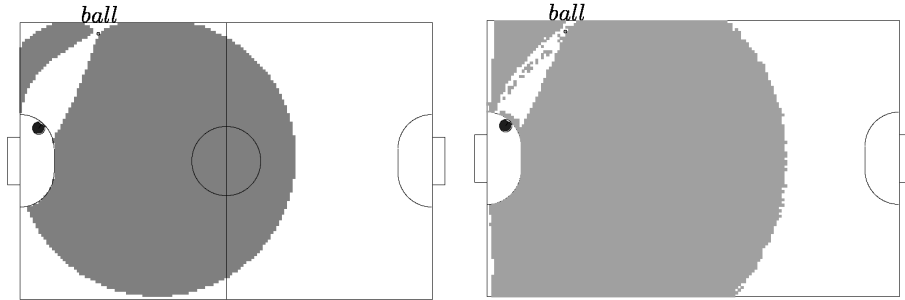


Fig. 19. Safety region: one defence robot case **Fig. 20.** Safety region: simulation result corresponding to Fig. 19

robots case under the RoboDragons’s defense strategy. Figures 19 through 22 show the examples of the experimental results.

In the figures, the white region is a safety region and the gray region is an unsafety region except the defense area in which the goalkeeper stands. There are two large gray areas in the field and the shapes of each area are similar between the proposed and simulated results. However, the down-left corner of the field does not match between the approximate results and the simulation results. (In the simulated result, there are many small gray dot-like areas. This is caused by the noise model implemented in the simulator.) These figures show that the approximate safety region is a well approximation of the safety region and can use as the safety region.

To show how much portion of safety and unsafety regions coincide with between the approximate method and the simulation, we define a coincidence rate R by the following equation.

$$R = \frac{\text{number of coincident points}}{\text{number of all points on the mesh}}, \quad (11)$$

where coincident points are points that the results of approximate method and simulation coincide with. Table 4 shows the result which is the average of 10 trials.

Computation time Using the three typical computers, we obtained the computation time for the proposed method. Table 5 shows the result.

In our system, given time for the computation of the safety region is at most 5 msec from our experience of the development of the RoboDragons system when we use the safety region in strategy computation in real time. From Table 5, we can realize the real time computation using the Xeon processor.

¹¹ We assume that the robot can kick the ball toward any direction.

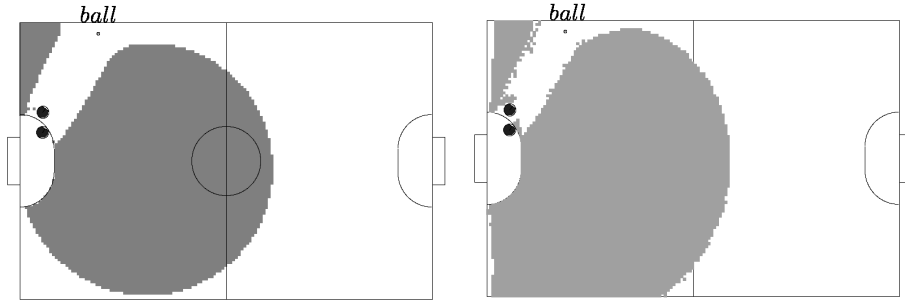


Fig. 21. Safety region: two defence robots **Fig. 22.** Safety region: simulation result corresponding to Fig. 21

Table 4. Coincidence rate (Direct play[2])

	coincidence rate R
one defence robot	0.889
two defence robots	0.869

10 A defence strategy using the safety region

In this section, we propose a defence strategy using the safety region against the cooperative play.

10.1 A defence algorithm using the safety region against the direct play

When n robots have already placed in defence positions and $(n + 1)$ th robot is placed in defence position, the following algorithm determines the position of the $(n + 1)$ th robot.

1. Letting the positions of n defence robots be \mathbf{r}_i ($i = 1, \dots, n$), obtain the safety region and the unsafety region. Number each connected component in the unsafety region. Let it be N_k ($k = 1, \dots$)

Table 5. Computation time

CPU	Memory	one defence robot	two defence robots
Pentium 4 2.8GHz	1 GB	4.5 msec	5.6 msec
Athron64 X2 4200+	512 MB	4.6 msec	6.1 msec
Xeon 3.3 GHz	2 GB	1.5 msec	1.9 msec

2. Search a connected component with maximal area (N_m) and compute the gravity center \mathbf{G} of N_m .
3. Place $(n + 1)$ th robot at the cross-point of the line L_g and the defence line (a bit outside of defence area), where L_g is a bisector line of the maximal free angle toward the goal from point \mathbf{G} .

Figures 23 and 24 are examples of the deployment of a new robot. Fig. 23 is obtained from Fig. 19 and Fig. 24 is obtained from Fig. 21. Figure 25 is the deployment of the three defence robots under the RoboDragons' existing strategy. Table 6 shows the number of points in the unsafety region.

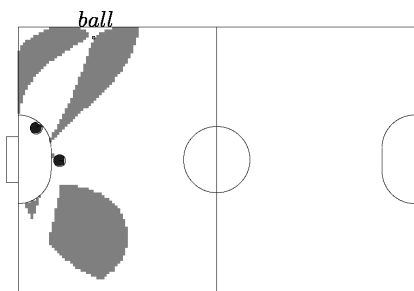


Fig. 23. Safety Region: Placing a new defence robot to figure 19

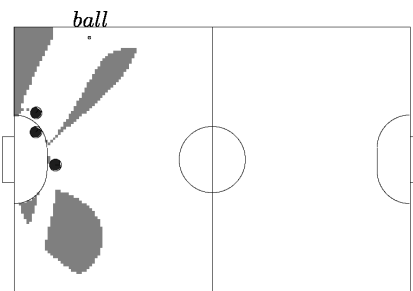


Fig. 24. Safety Region: Placing a new defence robot to figure 21

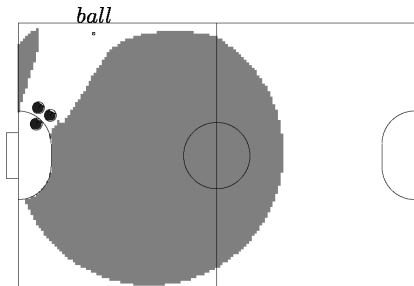


Fig. 25. Safety Region: Three defence robots (existing strategy)

From Table 6, it is shown that the proposed defence strategy (deployment algorithm) greatly reduces the area of the unsafety region. This means that it is possible to keep the goal to the great extent and shows that the proposed strategy is efficient against the opponent's cooperative play.

Table 6. the number of points in the unsafety region

	two defence robots	three defence robots
existing strategy	6256 (Fig. 21)	7086 (Fig. 25)
proposed strategy	1627 (Fig. 23)	1126 (Fig. 24)

However, the proposed defence strategy is not always efficient against the opponent's cooperative play. For example, applying the proposed strategy to Figure 26, we get Figure 27.

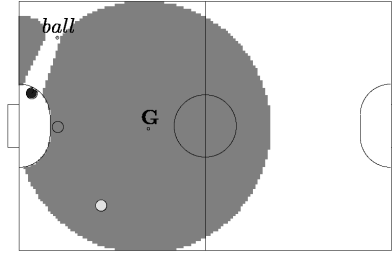


Fig. 26. Safety region: one defence robot

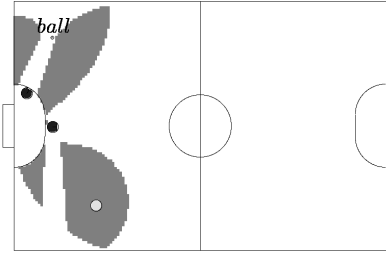


Fig. 27. Safety region: two defence robots

In Fig. 27, if the shooting robot is in the unsafety region which is shown by the circle in Fig. 27, the goal is achieved by the robot. This situation is not preferable. In the next section, we discuss how we avoid such situation.

10.2 A defence strategy considering the position of the opponent robot

In a real game, we should take the position of opponent robot into account. In this section, we discuss the weighted unsafety region. The weight is given to each point \mathbf{e} in the unsafety region as a function of the distance between the position of the opponent robot \mathbf{r}_e in the unsafety region and the point \mathbf{e} . We gave the following weighting function,

$$w(\mathbf{e}) = \max(1, 100 \times (1 - \frac{\|\mathbf{r}_e - \mathbf{e}\|}{\max(M, t_p \times v_r)})). \quad (12)$$

In eq. (12), v_r is a velocity of opponent robot at \mathbf{r}_e , and t_p is given by eq. (8). M is a threshold value to keep the weighting area wide when the value $t_p \times v_r$

is small. We used $M = 270$ in the experiment. $w(\mathbf{e})$ takes the value in the range between 1 and 100.

Computing the weighted gravity center \mathbf{G}' of the unsafety region, and replacing \mathbf{G} in the previous algorithm into \mathbf{G}' , we get an improved algorithm for

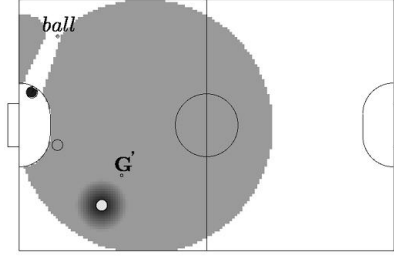


Fig. 28. Weighted unsafety region

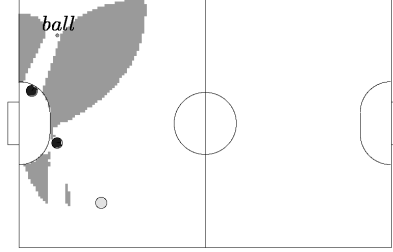


Fig. 29. Improved safety region

Table 7. Computation time of weighted (un)safety region

CPU	Memory	Weighted gravity center	Weighted (un)safety region
Pentium4 2.8 GHz	1 GB	1.0 msec	5.6 msec
Athron64 X2 4200+	512 MB	1.9 msec	6.4 msec
Xeon 3.3 GHz	2 GB	0.3 msec	1.9 msec

Figure 28 shows a weighted unsafety region. The higher the weight, the darker the region. The weighted gravity center comes near the opponent robot in the unsafety region. Figure 29 shows obtained defence positions of the robots and an improved safety region. From the Fig. 29, it is clear that the opponent robot is in the outside of the unsafety region.

The computation time of the weighted gravity center and weighted (un)safety region¹² excluding the computation of weighted gravity center are given in Table 7. Comparing Tables 5 with 7, it is shown the increase of computation time by the weighted (un)safety region is small and the real time computation is possible.

¹² When stating computation time, we use the term “weighted (un)safety region”, since it includes the computation time of both safety and weighted unsafety region.

11 Concluding remarks

In this paper, we describe the configuration of the RoboDragons' new robots. The robot is driven by four DC brushless motors. A new control board is developed. There is not a large improvement in the software of the RoboDragons this year. A minor improvement is described. Research topics which will be embedded in the future RoboDragons system are described. The dominant region method and the safety region method. These can be used for realising a higher strategy.

acknowledgement

This work was supported by the chief director's special study fund of Aichi Prefectural University and the president's special study fund of Aichi Prefectural University.

References

1. "<http://www.toppers.jp/en/index.html>"
2. Ryota Nakanishi, James Bruce, Kazuhito Murakami, Tadashi Naruse and Manuela Veloso, "Cooperative 3-Robot Passing and Shooting in the RoboCupSmall Size League", RoboCup 2006: Robot Soccer World Cup X, LNCS 4434 pp.418-425
3. K. Murakami, S. Hibino, Y. Kodama, T. Iida, K. Kato and T. Naruse "Cooperative Soccer Play by Real Small-Size Robot", In RoboCup 2003: Robot Soccer World Cup VII, LNAI3020, pp. 410 - 421, Springer-Verlag, 2003
4. F.P. Preparata and M.I. Shamos "Computational Geometry" Springer, 1988
5. T. Taki and J. Hasegawa "Dominant Region: A Basic Feature for Group Motion Analysis and Its Application to Teamwork Evaluation in Soccer Games", Proc. SPIE Conference on Videometrics VI, Vol.3641, Pp.48-57 (Jan. 1999)
6. R. Nakanishi, K. Murakami and T. Naruse "Dynamic Positioning Method Based on Dominant Region Diagram to Realize Successful Cooperative Play", In RoboCup 2007: Robot Soccer World Cup XI, LNAI5001, pp. 488 - 495, Springer-Verlag, 2007
7. H. Achiwa, J. Maeno, J. Tamaki, S. Suzuki, T. Moribayasi, K. Murakami and T. Naruse "RoboDragons 2009 Extended Team Description", http://small-size.informatik.uni-bremen.de/tdp/etdp2009/small_robotdragons.pdf